



## Research papers

## Nitrate sources and transformations in a river-reservoir system: Response to extreme flooding and various land use

Xingchen Zhao<sup>a,b</sup>, Hai Xu<sup>a,\*</sup>, Lijuan Kang<sup>a</sup>, Guangwei Zhu<sup>a</sup>, Hans W. Paerl<sup>c</sup>, Huiyun Li<sup>a</sup>,  
Mingliang Liu<sup>d</sup>, Mengyuan Zhu<sup>a</sup>, Wei Zou<sup>a</sup>, Boqiang Qin<sup>a</sup>, Yunlin Zhang<sup>a</sup>

<sup>a</sup> Key Laboratory of Lake and Watershed Science for Water Security, Nanjing Institute of Geography & Limnology, Chinese Academy of Sciences, 73 East Beijing Road, Nanjing 210008, China

<sup>b</sup> School of Geography and Ocean Science, Nanjing University, Nanjing, Jiangsu Province 210023, China

<sup>c</sup> Institute of Marine Sciences, University of North Carolina at Chapel Hill, 3431 Arendell Street, Morehead City, NC 28557, USA

<sup>d</sup> Hangzhou Institute of Ecological and Environmental Sciences, Hangzhou 310005, China

## ARTICLE INFO

This manuscript was handled by Yuefei Huang, Editor-in-Chief, with the assistance of Bing Li, Associate Editor

## Keywords:

$\delta^{15}\text{N}$

$\delta^{18}\text{O}$

Nitrate source apportionment

River-reservoir system

Flooding

Lake Qiandao

## ABSTRACT

Nitrate ( $\text{NO}_3^-$ ) pollution poses a global aquatic threat, promoting eutrophication and endangering human health. Large floods can swiftly drive significant nitrogen load into rivers and downstream water bodies, nevertheless, precisely quantifying  $\text{NO}_3^-$  sources in watersheds with complex land use patterns remains challenging. In June 2020, heavy and persistent rainfall triggered severe floods across southeastern China, causing Lake Qiandao, the largest reservoir in this region, to reach its highest recorded level. This study investigated  $\text{NO}_3^-$  sources and transformations within the Xin'an River-Lake Qiandao system, particularly focusing on the impact of the catastrophic summer flooding event. Through extensive sampling, we identified a distinct nitrogen concentration gradient: from the pristine Xin'an River source, characterized by 95 % forest cover and consistently low nitrogen levels for the initial 125 km, to a gradual rise as the river traversed human-impacted regions, culminating in peak concentrations within residential and agricultural areas. Isotopic analysis identified a general upward trend in nitrate stable isotope ( $\delta^{15}\text{N}\text{-NO}_3^-$ ) associated with the expansion of agricultural and urban lands. Mean values of  $\delta^{15}\text{N}\text{-NO}_3^-$  gradually increased from headwaters and forest-dominant catchments (+2.88 ‰) to agricultural regions (+6.64 ‰) and residential areas (+7.10 ‰). A Bayesian modeling identified that during the flood season, soil erosion and chemical fertilizers were the primary contributors, collectively accounting for 74 % of  $\text{NO}_3^-$  sources in the Xin'an River. However, accumulated sewage in tributaries and the overflow of sewage from treatment plants, exacerbated by the flood, significantly impacted Lake Qiandao, particularly in densely populated urban areas, contributing 53 % of the total  $\text{NO}_3^-$  input. Additionally,  $\text{NO}_3^-$  levels and isotopic values in Lake Qiandao were influenced by a mixture of sources and nitrogen cycling processes, including nitrification and algae assimilation following the flood event. In contrast, during baseflow conditions, the contribution of domestic sewage and livestock wastewaters increased to 41 % in the upper river, while Lake Qiandao remained affected by non-point source pollution, with soil erosion and chemical fertilizers contributing 58 % to the total nitrogen pollution. This study sheds light on the complex dynamics of  $\text{NO}_3^-$  dynamics within river-reservoir systems, particularly in the context of extreme flooding, emphasizing the critical need for comprehensive water quality management strategies along the entire watershed.

### 1. Introduction

Reservoirs, created by damming rivers, have fragmented over 50 % of global waterways for purposes like hydropower production, flood control, navigation, and drinking water supplies (Grill et al., 2019; Yang et al., 2021). Human activities, dramatically increasing in the past

century, significantly contribute to nitrogen (N) enrichment in water bodies, primarily through agricultural over-fertilization and poor timing of fertilizer applications (Galloway et al., 2004). Intensified precipitation and flooding have further exacerbated sediment and nutrient transport from land to water systems (Keys et al., 2019; Neville et al., 2021; Yue et al., 2020), leading to increased sedimentation in global

\* Corresponding author.

E-mail address: [hxu@niglas.ac.cn](mailto:hxu@niglas.ac.cn) (H. Xu).

<https://doi.org/10.1016/j.jhydrol.2024.131491>

Received 23 October 2023; Received in revised form 18 April 2024; Accepted 27 May 2024

Available online 17 June 2024

0022-1694/© 2024 Published by Elsevier B.V.

reservoirs and a consequent reduction in their storage capacity (Graf et al., 2010; Kondolf et al., 2014). Elevated N loading, mainly in the form of highly soluble nitrate ( $\text{NO}_3^-$ ), has accelerated eutrophication, triggered harmful algal blooms, deteriorated water quality, and posed substantial risks to human health (Ho et al., 2019; Nieder et al., 2018; Qin et al., 2021; Xia et al., 2017). Moreover, forthcoming climate changes are anticipated to further impact the transformation and retention of nitrogen in rivers and reservoirs (Seneviratne et al., 2021). Given this increasingly dynamic situation, effective water quality management requires identification and quantification of N sources and understanding transport and transformation processes driving local nitrate concentrations.

Isotopes offer a direct method to discern nitrate sources due to their distinct isotopic compositions (Xue et al., 2009; Yue et al., 2020; Zhang et al., 2014). Additionally, biological nitrogen cycling yields predictable changes in isotopic ratios (Kendall, 1998; Mariotti et al., 1984; Voss et al., 2006). Processes like microbial  $\text{N}_2$  fixation and ammonification typically exhibit negligible fractionation, while other transformations, such as nitrification and denitrification, cause significant isotopic shifts (Böttcher et al., 1990; Granger and Wankel, 2016). A Bayesian model (stable isotope analysis in R, SIAR) ran under an open-source statistical software R, addresses persistent issues unhandled by simpler mixing models (Parnell et al., 2010). SIAR excels in apportioning over three sources using only two isotopes, considering source ranges and distributions. Additionally, SIAR can incorporate fractionation effects and provide complete posterior distributions for various  $\text{NO}_3^-$  source contributions, yielding various statistics (variance, mean value, quintiles) from these distributions (Davis et al., 2015; Xia et al., 2019; Zhang et al., 2018).

Previous investigations on nitrate sources in lakes and reservoirs have primarily focused on the water body itself (Jin et al., 2019; Wang, 2020; Wang et al., 2020) or its inlet (Cui et al., 2020; Jin et al., 2015; Yi et al., 2017), often omitting simultaneous comparisons with inflowing rivers. This restricted approach may lead to an inadequate and biased understanding of nitrate pollution sources and transport processes. A comprehensive understanding necessitates monitoring nitrate concentrations and isotopic compositions in both inflowing rivers and receiving lakes and reservoirs.

This study focuses on the Lake Qiandao basin, home to the largest reservoir (580  $\text{km}^2$ ) in southeastern China, which serves as the drinking water source for 10 million inhabitants (Zhu et al., 2022). The Xin'an River, the main inflow to Lake Qiandao, significantly contributes to its discharge (60 %) (Chen et al., 2020a) and nitrogen loads (70 %) (Li et al., 2022). Unfortunately, the diverse land uses in the Xin'an River catchment, including native forests, agriculture, rural, and urbanized areas, introduce nitrogen pollutants such as soil erosion, synthetic fertilizer, livestock waste, and sewage effluent (Pueppke et al., 2019). These pollutants pose a threat to the water quality of Lake Qiandao. Recent research has highlighted the increasing threats of eutrophication and harmful algal bloom events in Lake Qiandao (Zhu et al., 2022) in the context of growing urban and agricultural wastewater impacts, and increased rainstorm frequency (Li et al., 2020b; Zhou et al., 2020). Therefore, accurately identifying nitrate sources in both the mainstream and lake is crucial to safeguard lake's water quality.

The primary objective was to comprehensively understand nitrate dynamics and sources in the Xin'an River-Lake Qiandao system, with a specific focus on data of summer flood period compared to other seasons. Through this comparative analysis and employing nitrate isotopes, we aimed to unveil sources, transformation processes, and the influence of the extreme flood on nitrate migration. Our research highlighted the importance of identifying nitrate origins to safeguard Lake Qiandao's water quality and offered insights into the impact of land use and extreme flooding. By exploring isotopic variations and cycling mechanisms, this study contributed to more effective water resource management and pollution control, ensuring the sustainability of this vital aquatic ecosystem.

## 2. Material and methods

### 2.1. Study area

Lake Qiandao, also known as Xin'anjiang Reservoir, is a deep (mean depth = 30 m) and large (storage capacity =  $17.8 \times 10^9 \text{ m}^3$ ) water body located in Chun'an County, Zhejiang Province, China (Fig. 1). The entire watershed features steep slopes and thin, easily erodible soils. Forest land covers approximately 70 % of the upper reaches of Xin'an River and Chun'an County. Farmland and residential areas are mainly distributed in the middle and lower plains along Xin'an River, as well as the northeast and southwest tributaries of Lake Qiandao (Fig. 1). With an annual soil erosion rate of  $3.21 \times 10^5 \text{ kg} \cdot \text{km}^{-2} \cdot \text{yr}^{-1}$ , the region is classified as slightly eroded based on the soil erosion criteria (SL190-2007 standard in China) (Wang et al., 2023). Tea plantations, covering 4.5 % of the total area, are notable features in the watershed. Based on the Huangshan Statistical Yearbooks (2023), the application of chemical fertilizers in the Xin'an River basin reached 537  $\text{kg}/\text{ha}$  in 2022, a rate 2.5 times higher than that in developed countries and significantly exceeds the national average ( $375 \text{ kg} \cdot \text{ha}^{-2} \cdot \text{y}^{-1}$ ). Additionally, manure derived from scatter-feed livestock (chickens, ducks, geese, and pigs), is periodically spread throughout the year. The other two primary  $\text{NO}_3^-$  sources in river and reservoir waters are atmospheric deposition (wet deposition, AD), and nitrate derived from mineralization and nitrification of organic soil nitrogen (SN).

The region experiences a typical subtropical humid monsoon climate. The wet season, occurring from June to September, accounts for about 42 % of the total rainfall (Li et al., 2022). In July 2020, the area experienced its most catastrophic summer flooding since at least 1998, caused by a series of heavy rains from June into July. This event impacted extensive areas of southern China, including the Yangtze River and its tributaries (Li et al., 2020a). Certain parts of the Xin'an River basin received continuous precipitation exceeding 10  $\text{mm}/\text{h}$  for 10 h from July 6 to July 7, 2020. Peak instantaneous discharge exceeded 1 000  $\text{m}^3/\text{s}$  (Fig. S1), leading to the Qiandao Lake reaching its highest recorded level and the unprecedented full opening of all 9 gates of the dam for flood discharge.

### 2.2. Field sampling

The study comprised 67 sampling sites, 33 of which were located in the Xin'an River and 34 distributed across various regions of Lake Qiandao (Fig. 1). These river sampling sites represented a diverse range of land uses, including undisturbed mountainous regions, forests, settlement areas, and those impacted by anthropogenic factors such as wastewater and agricultural land use. For specific information concerning sampling sites, please refer to the Text S1. Sampling campaigns were conducted to capture seasonal variations and an extreme flood event's impact on nitrogen migration and cycling. One sampling occurred during the high flow season in July 2020, while three additional samplings were done in late October 2020, January 2021, and April 2021 during the low flow seasons.

In-situ measurements of water temperature (WT), pH, and dissolved oxygen (DO) were taken using an EXO multi-parameter water-quality analyzer. Water samples were collected at 20 cm depth in the middle of Xin'an River and at the surface layers (0.5 m below the surface) at Lake Qiandao sites. Approximately 100 mL of raw water samples were directly collected into pre-cleaned polyethylene bottles and subsequently frozen at  $-20 \text{ }^\circ\text{C}$  until the determination of total nitrogen (TN) concentration. Additionally, 500 mL of water samples were filtered through 0.22  $\mu\text{m}$  Whatman GF/F membrane filters, and the resulting filtrate was also frozen at  $-20 \text{ }^\circ\text{C}$  for subsequent analysis.

### 2.3. Water quality and stable isotope analysis

In the laboratory, TN concentration was measured

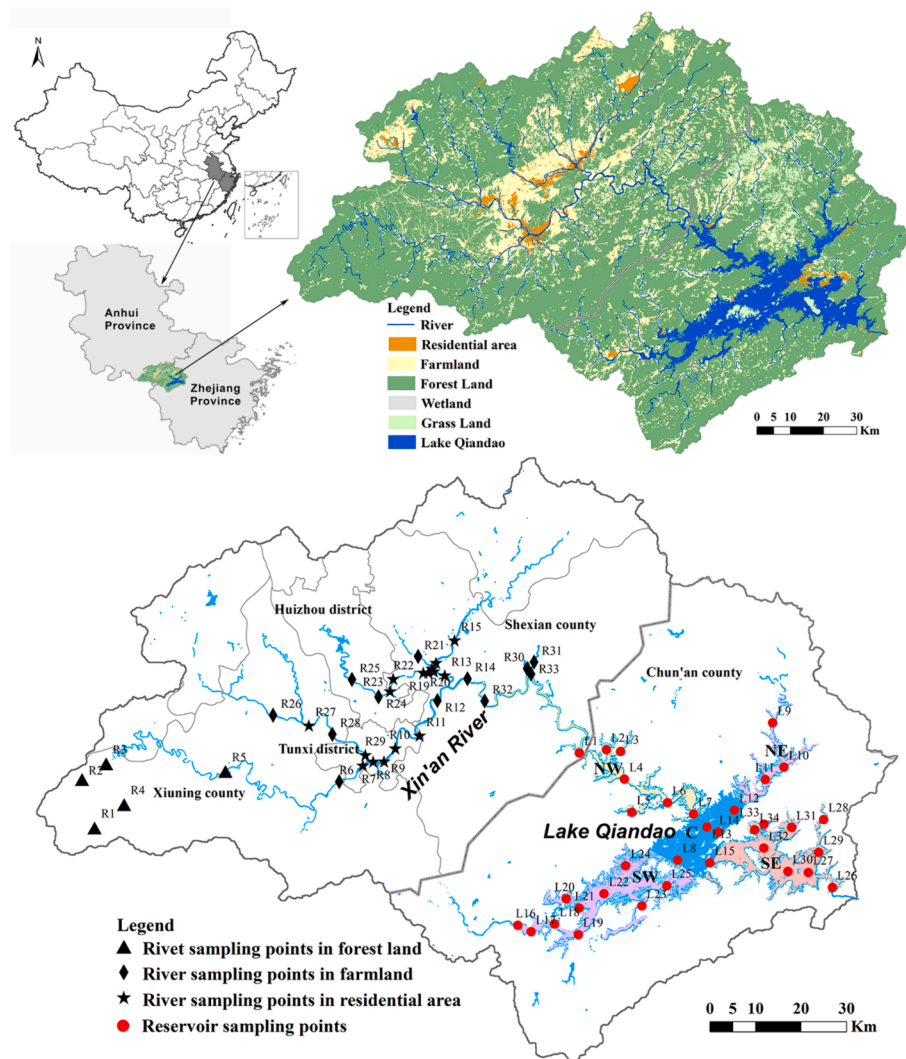


**Fig. 1.** Geographic location and sampling sites of Xin'an River and Lake Qiandao. NW, NE, SW, SE, and C representing the northwest, northeast, southwest, southeast, and central regions of Lake Qiandao, respectively.

spectrophotometrically after digestion with alkaline potassium persulfate. The filtrate for  $\text{NO}_3^-$ -N and  $\text{NH}_4^+$ -N concentrations was analyzed photometrically on a continuous flow analyzer (Skalar San<sup>++</sup>, the Netherlands), chloride ( $\text{Cl}^-$ ) concentration was measured using ion chromatography (ICS-1100, Dionex, USA). Chlorophyll *a* concentration (Chl *a*) was extracted from GF/F filters with hot 90 % ethanol and measured by spectrophotometry (Jin and Tu, 1990). Suspended particulate matter (SPM) was categorized into inorganic (SPIM) and organic (SPOM) parts, with weights determined using a weighing method (Liu et al., 2019). Phytoplankton samples were collected and immediately preserved in Lugol's iodine solution (1 %, V/V). After sedimentation for at least 24 h, algal species were counted under an Olympus BX53 microscope. The phytoplankton density and biomass were identified according to the methods described by (Guo et al., 2019).

The values of  $\delta\text{D}-\text{H}_2\text{O}$  and  $\delta^{18}\text{O}-\text{H}_2\text{O}$  were analyzed using an isotope ratio mass spectrometer (Thermo Mat 253 Plus) at the State Key Laboratory of Lake Science and Environment in Nanjing Institute of Geography and Limnology. The international calibration materials of Vienna Standard Mean Ocean Water (VSMOW) were used for correction. For  $\delta^{15}\text{N}-\text{NO}_3^-$  and  $\delta^{18}\text{O}-\text{NO}_3^-$  analysis, the ammonium-zinc-cadmium reduction method was employed to convert nitrate to nitrous oxide (Li et al., 2021; McIlvin and Altabet, 2005), and the resulting gases were analyzed using isotope ratio mass spectrometry via Gasbench II (Gashench-DELTA<sup>plus</sup> XP; Thermo-Finnigan, USA) at the Third Institute

of Oceanography, Ministry of National Resources, China. All stable isotope results are expressed as  $\delta$  values, representing deviations in permil (‰) relative to atmospheric  $\text{N}_2$  and Vienna Standard Mean Ocean Water (VSMOW):

$$\delta(\%) = \left[ \frac{R_{\text{sample}} - R_{\text{standard}}}{R_{\text{standard}}} \right] \times 1000 \quad (1)$$

where  $R_{\text{sample}}$  and  $R_{\text{standard}}$  are the isotopic ratio (e.g., D/H,  $^{15}\text{N}/^{14}\text{N}$  or  $^{18}\text{O}/^{16}\text{O}$ ) of the measured sample and standard, respectively. The reference ratio of  $^{15}\text{N}/^{14}\text{N}$  is  $\text{N}_2$  in air, the D/H and  $^{18}\text{O}/^{16}\text{O}$  reference is VSMOW. Two international reference materials, USGS-32 and USGS-34 were utilized for calibration.  $\delta > 0$  indicates that the heavy isotopes in the sample are more abundant than the standard; conversely, it means that the sample is deficient in heavy isotopes.

#### 2.4. Nitrate source contributions quantification and isotopic fractionation integration

To estimate the proportion of  $\text{NO}_3^-$  source contributions, we employed Bayesian stable isotope mixing models based on the approach described in Parnell et al. (2010). This modeling, implemented using the "SIAR" (Stable Isotope Analysis in R) package, allows us to consider more than two sources and incorporate fractionation effects, as demonstrated in previous studies (Parnell et al., 2010; Xue et al., 2012).

For the characterization of potential source isotopic compositions (Table S1), we conducted a comprehensive survey and collected samples of precipitation, soil, chemical fertilizers, manure, and sewage. Seven precipitation samples were collected from the meteorological observation station in Chun'an County, Weiping Town, between November 2020 and February 2021. Additionally, six sewage samples were collected, comprising untreated wastewater from the influents of urban sewage treatment plants and domestic wastewater from residential properties along the riverbanks.

To improve calculation precision, we incorporated isotopic fractionation in our modeling. According to the Rayleigh equation, biological N removal can be identified by a negative linear correlation between the isotope values and  $\ln(N)$  (Jiang et al., 2021). The isotopic enrichment factor ( $\epsilon$ ) during  $\text{NO}_3^-$  assimilation or denitrification process can be obtained from the slope of the relationship between dual nitrate isotopes and  $\ln(\text{NO}_3^-)$  (Chen et al., 2020b; Yue et al., 2020).

SIAR produces an extensive set of realizations representing the proportional contributions of sources using Markov Chain Monte Carlo (MCMC) (Parnell et al., 2010). The properties of posterior probability distributions of the source contributions (e.g., the mean, standard deviation, and quartiles et al.) can be obtained via analyzing these generated realizations.

### 3. Results

#### 3.1. Spatial and temporal variations in nitrogen concentrations

Originating from the pristine headwaters of the Xin'an River, characterized by 95 % forest cover and minimal human impact, the Xin'an River-Lake Qiandao system displayed a clear nitrogen concentration gradient (Fig. 2).  $\text{NO}_3^-$ -N was the dominant form of dissolved inorganic nitrogen (DIN, comprising  $\text{NO}_3^-$ -N and  $\text{NH}_4^+$ -N), accounting for 60 % of total DIN in both the Xin'an River and Lake Qiandao waters during the sampling period. Nitrogen concentrations were lowest at the Xin'an River's source (TN:  $0.65 \pm 0.04$  mg/L (average  $\pm$  S.E.);  $\text{NO}_3^-$ -N:  $0.39 \pm 0.15$  mg/L) (Table S2, Fig. 2a) and remained constantly low along the first 125 km forested-section. Following that, nitrogen levels steadily increased as the river passed through regions impacted by human activities, reaching their peak in residential areas (TN:  $1.90 \pm 0.91$  mg/L;  $\text{NO}_3^-$ -N:  $0.99 \pm 0.40$  mg/L) and agricultural land use (TN:  $1.47 \pm 0.55$  mg/L;  $\text{NO}_3^-$ -N:  $0.94 \pm 0.44$  mg/L). Notably, the highest TN concentrations were observed in residential regions, reaching up to 5.70 mg/L, while agricultural lands exhibited the highest  $\text{NO}_3^-$ -N levels at 1.99 mg/L. Subsequently, as the water transitioned from the river to the reservoir, nitrogen concentrations exhibited a gradual decline along the main flow, from the inflow northwestern region (TN:  $1.31 \pm 0.42$  mg/L;  $\text{NO}_3^-$ -N:  $0.75 \pm 0.35$  mg/L) to the southeastern region just before the

dam (TN:  $0.78 \pm 0.10$  mg/L;  $\text{NO}_3^-$ -N:  $0.50 \pm 0.26$  mg/L). Overall,  $\text{NO}_3^-$ -N concentrations increased by 75 % from headwater to the river-reservoir breakpoint.

In addition to assessing spatial nitrogen distribution, our study revealed a distinct seasonal pattern (Table S2; Fig. 2b). Nitrogen levels in the Xin'an River increased from spring to summer, notably peaking following the July 2020 flood event (TN:  $1.63 \pm 0.71$  mg/L;  $\text{NO}_3^-$ -N:  $0.97 \pm 0.46$  mg/L), comparable to those observed during winter (TN:  $1.96 \pm 1.24$  mg/L;  $\text{NO}_3^-$ -N:  $0.98 \pm 0.53$  mg/L). Autumn exhibited the lowest concentrations (TN:  $1.27 \pm 0.64$  mg/L;  $\text{NO}_3^-$ -N:  $0.70 \pm 0.38$  mg/L). In contrast, during Lake Qiandao's flood periods, nitrogen concentrations remained relatively low (TN:  $0.83 \pm 0.33$  mg/L;  $\text{NO}_3^-$ -N:  $0.34 \pm 0.30$  mg/L) compared to the elevated levels observed in spring and winter (TN averaging 0.98 mg/L;  $\text{NO}_3^-$ -N averaging 0.70 mg/L).

#### 3.2. Isotopic characteristics of nitrate

The nitrate isotopic compositions ( $\delta^{15}\text{N}-\text{NO}_3^-$  and  $\delta^{18}\text{O}-\text{NO}_3^-$ ) of samples from the Xin'an River and Lake Qiandao exhibited significant variations during the investigation period (Table S2, Fig. 3 and Fig. 4). Land use strongly influenced nitrate isotopic patterns and sources within the Xin'an River basin (Table S2 and Fig. S2). Mean and maximal values of  $\delta^{15}\text{N}-\text{NO}_3^-$  gradually increased from forests (+2.88 ‰ and +8.71 ‰) to agricultural regions (+6.64 ‰ and +14.02 ‰) and residential areas (+7.10 ‰ and +15.22 ‰) (Fig. S2). Conversely, the means of  $\delta^{18}\text{O}-\text{NO}_3^-$  remained relatively consistent, measuring 4.24 ‰, 2.52 ‰, and 2.80 ‰ for forested land, farmland, and residential areas respectively. Regarding Lake Qiandao, its isotopic values in the northwest and northeast regions resembled those in the lower reaches of the Xin'an River, while the isotopic values in the central and southern lakes generally showed enrichment compared to those in the Xin'an River and the northern lakes (Table S2).

The isotopic data following the flood event exhibited distinctive variations compared to other periods (Fig. 3). During the flood season, there was relatively limited overlap in the  $\delta^{15}\text{N}-\text{NO}_3^-$  and  $\delta^{18}\text{O}-\text{NO}_3^-$  values between the Xin'an River and Lake Qiandao, with significantly higher values observed in the central and southern regions of Lake Qiandao compared to the Xin'an River ( $p < 0.01$ ). Additionally, during this season, the Xin'an River recorded its lowest annual lowest  $\delta^{15}\text{N}-\text{NO}_3^-$  and  $\delta^{18}\text{O}-\text{NO}_3^-$  levels ( $\delta^{15}\text{N}$ :  $5.10 \pm 5.27$  ‰;  $\delta^{18}\text{O}$ :  $-2.88 \pm 4.43$  ‰), while Lake Qiandao displayed its highest annual values for  $\delta^{15}\text{N}-\text{NO}_3^-$  and  $\delta^{18}\text{O}-\text{NO}_3^-$  ( $\delta^{15}\text{N}$ :  $9.56 \pm 3.32$  ‰;  $\delta^{18}\text{O}$ :  $5.93 \pm 4.32$  ‰) (Fig. 3). These elevated values in Lake Qiandao implied distinct nitrate sources and transport patterns compared to the Xin'an River. In contrast, during other seasons, both the Xin'an River and Lake Qiandao exhibited narrower overall ranges in  $\delta^{15}\text{N}-\text{NO}_3^-$  and  $\delta^{18}\text{O}-\text{NO}_3^-$  values compared to the flood season.

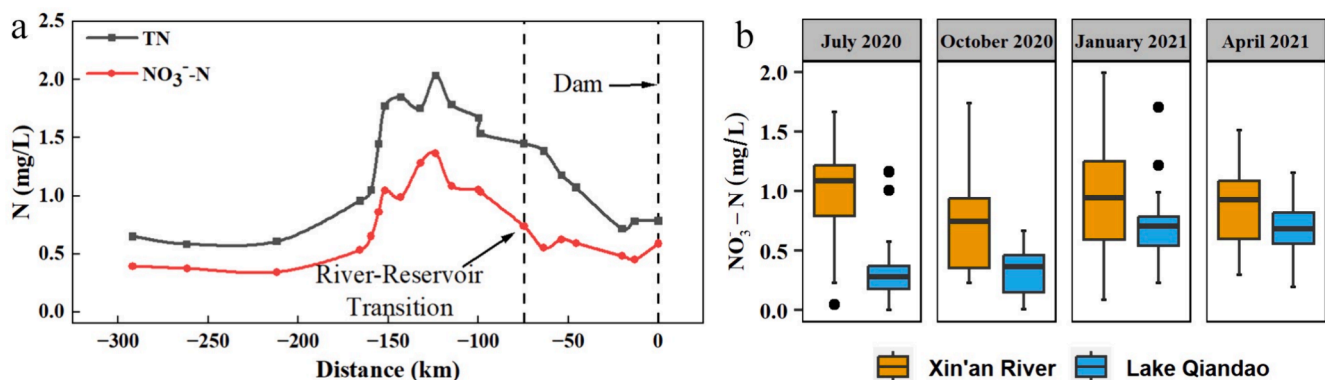


Fig. 2. Longitudinal trends in mean TN and  $\text{NO}_3^-$ -N concentrations along the Xin'an River to Lake Qiandao, averaged across four seasons (July 2020, October 2020, January 2021, and April 2021) (a). Seasonal variations in  $\text{NO}_3^-$ -N concentrations between the Xin'an River and Lake Qiandao (b). Box plots illustrate the 25th, 50th and 75th percentile; the whiskers indicate the 2.5th and 97.5th percentiles; and the points represent data outliers.

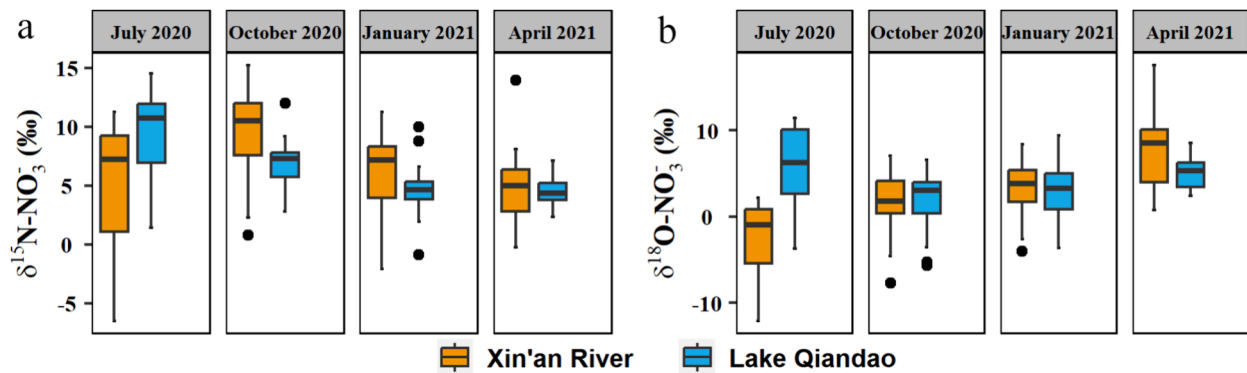


Fig. 3. Seasonal variations in  $\delta^{15}\text{N-NO}_3^-$  (a) and  $\delta^{18}\text{O-NO}_3^-$  (b) between the Xin'an River and Lake Qiandao.

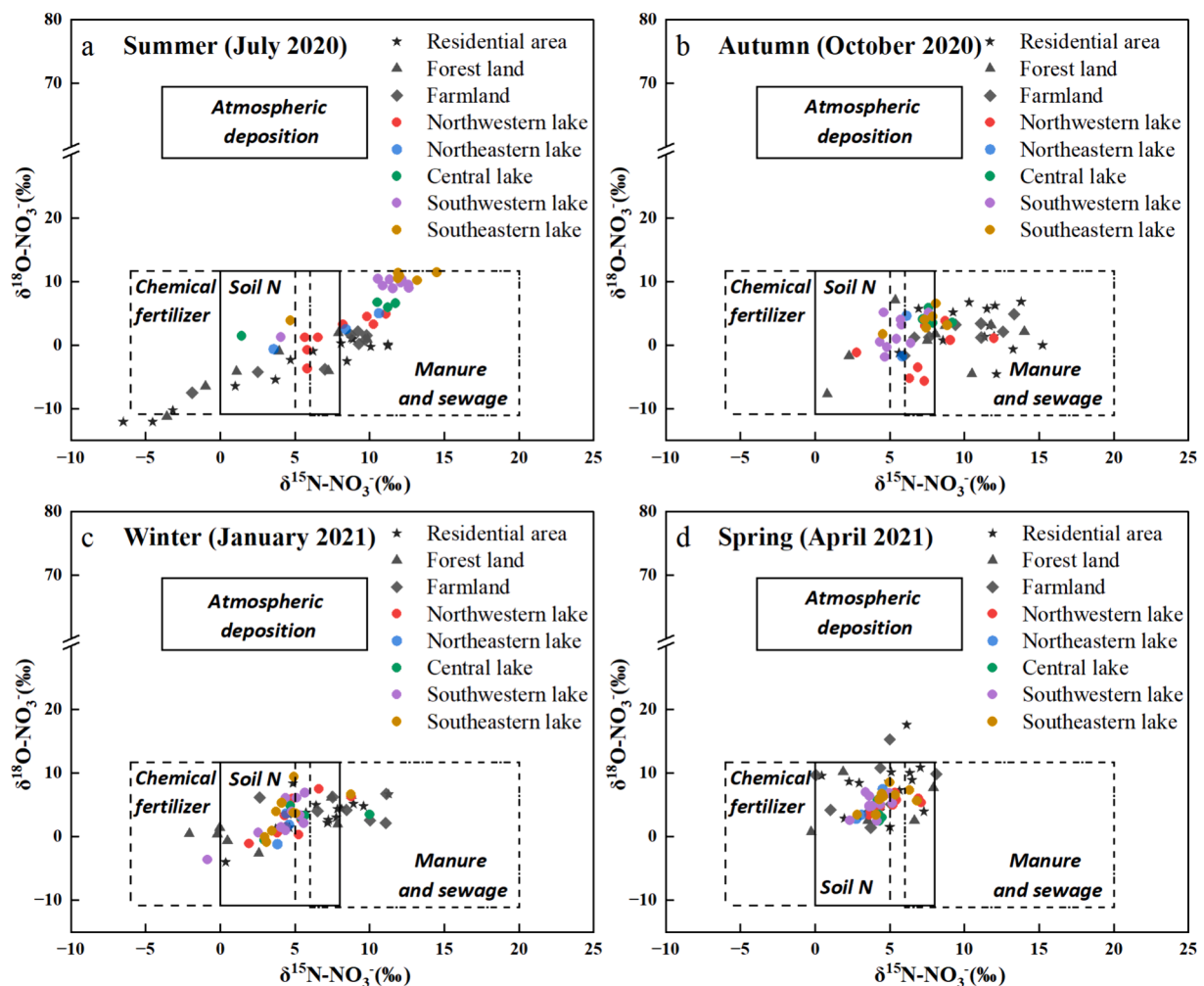


Fig. 4. Scatterplot of  $\delta^{15}\text{N-NO}_3^-$  and  $\delta^{18}\text{O-NO}_3^-$  values in the Xin'an River and Lake Qiandao. The  $\delta^{15}\text{N-NO}_3^-$  and  $\delta^{18}\text{O-NO}_3^-$  values in each source ( $\text{NO}_3^-$  in atmospheric deposition, chemical fertilizer, soil N, and manure and sewage) were summarized by Kendall et al. (2007) and Xue et al. (2009).

### 3.3. Isotopic characteristics of water

The variations in  $\delta^{18}\text{O}$  and  $\delta\text{D}$  values of water are depicted in Fig. S3, with the local meteoric water line (LMWL) derived from data obtained from local precipitation samples. During the June 2020 flood period, Lake Qiandao samples plotted on the upper right obviously deviated from the LMWL (Fig. S3a). This deviation may be associated with evaporation, since  $^{18}\text{O}$  enrichment surpasses that of deuterium during evaporation (Gonfiantini, 1986), consequently elevating oxygen and

hydrogen isotopic values and causing a systematic deviation from the LMWL (Hu et al., 2019b).

Moreover, the average  $\delta\text{D-H}_2\text{O}$  ( $-44.3\text{‰}$ ) and  $\delta^{18}\text{O-H}_2\text{O}$  ( $-7.0\text{‰}$ ) in Lake Qiandao water during the flood period were markedly higher than those in Xin'an River water ( $\delta\text{D-H}_2\text{O}$ :  $-52.2\text{‰}$ ;  $\delta^{18}\text{O-H}_2\text{O}$ :  $-8.2\text{‰}$ ) compared with other periods (Fig. S3). The distinct isotopic signatures between river and lake samples suggest that, besides the influx from the Xin'an River, a substantial portion of water during this period likely originates from alternative sources, such as surrounding

tributaries. Conversely, the overlapping water isotopic compositions between river and lake water during other sampling periods (Fig. S3) indicate that Xin'an River water constitutes a notable source for Lake Qiandao (Hu et al., 2019a).

#### 4. Discussion

##### 4.1. Land use impact on nitrate concentrations and isotopic variations in the Xin'an River basin

Our findings revealed notable spatio-temporal variations in  $\text{NO}_3^-$  concentrations and isotopic values, potentially linked to factors like land use types, anthropogenic activities, and storm events. This is in line with numerous prior studies that have demonstrated an increasing trend in exported nitrogen concentration and  $\delta^{15}\text{N}$  ratios corresponding to increased agricultural land, urbanization, and population density at the watershed-scale (Ding et al., 2014; Divers et al., 2014; Kaushal et al., 2011). In the Xin'an River basin, we also explored the relationship between mean nitrate isotopic signatures ( $\delta^{15}\text{N}/\delta^{18}\text{O}$ ) and the proportions of agricultural and residential land use (Fig. S2). Our analysis identified a general upward trend in  $\delta^{15}\text{N}-\text{NO}_3^-$  with expanding agricultural and urban lands (Fig. S2a). In contrast,  $\delta^{18}\text{O}-\text{NO}_3^-$  showed no significant correlation with major land use types (Fig. S2b). This may be due to  $\delta^{18}\text{O}-\text{NO}_3^-$  variations influenced by: 1) reactive isotope fractionation during nitrate formation, 2) temperature and hydrological conditions, or 3) minor yet variable direct atmospheric nitrate inputs into the river system (Mueller et al., 2016).

Headwaters and forest-dominant catchments exhibited  $\delta^{15}\text{N}-\text{NO}_3^-$  variation from 0.96 ‰ to 3.73 ‰ (Fig. 4), consistent with reported ranges for forested watersheds (−1‰ ~ 5‰) (Ding et al., 2022), and displayed low mean  $\text{NO}_3^-$ -N concentrations of 0.38 mg/L. However, forested catchments with over 20 % agricultural land-use showed a marked a positive  $\delta^{15}\text{N}-\text{NO}_3^-$  increase up to 5 ‰, indicating the influence of nitrogen sources associated with agricultural practices, like excessive application of organic manure and chemical fertilizers. Additionally, the semi-urban areas surrounding the sampling points along the Xin'an River featured mixed agricultural and residential land use. In regions with a higher proportion of agricultural land, elevated  $\text{NO}_3^-$  concentrations were likely attributed to local fertilizer and manure volatilization.

Chloride ( $\text{Cl}^-$ ) is a useful chemical indicator to distinguish between chemical fertilizer and domestic sewage sources. Its concentrations primarily change through mixing within the river system, due to its biological and chemical inertness (Ding et al., 2014; Yin et al., 2020). Notably, high levels of  $\text{Cl}^-$  and  $\delta^{15}\text{N}-\text{NO}_3^-$  values are typically observed in residential areas, where  $\text{Cl}^-$  may originate from anthropogenic sources, particularly sewage/manure and industrial/domestic waste (M&S). Additionally, chemical fertilizers used in the study area typically did not contain  $\text{Cl}^-$  (Yang et al., 2013). During the flood season, the observed lowest  $\text{Cl}^-$  concentrations (Table S2) both in the Xin'an River and Lake Qiandao water could be attributed to a significant increase in water volume (Xia et al., 2017), whereas the highest concentrations occurred in the fall and winter seasons, highlighting the increased M&S contribution during these seasons. Additionally, we noted slightly higher averaged  $\text{Cl}^-$  concentrations in the southwestern (2.49 mg/L) and central lake regions (3.39 mg/L), with the highest  $\delta^{15}\text{N}-\text{NO}_3^-$  values (10.87 ‰) identified in southwestern lake region during the flood period compared to other lake areas. The two regions are characterized by the most concentrated area of population distribution in the entire Lake Qiandao watershed. Residential areas consistently exhibited higher  $\text{Cl}^-$  concentrations than other land use types, particularly when compared to nearly pristine forested areas. Correspondingly, we also observed elevated  $\text{NO}_3^-$ -N concentrations (1.92 mg/L) and the highest  $\delta^{15}\text{N}-\text{NO}_3^-$  value (15.22 ‰) in the residential areas along the mid-to-lower Xin'an River sections, where the population is approximately 750,000, indicating that M&S had a greater impact on these waters.

##### 4.2. Nitrogen transformation processes in the river-reservoir system

Numerous previous studies have shown different  $\text{NO}_3^-$  isotopic compositions are influenced not only by diverse  $\text{NO}_3^-$  sources but also by nitrogen transformation processes (e.g., nitrification, assimilation and denitrification) (Chen et al., 2012; Mueller et al., 2016; Yang and Toor, 2016). According to Kendall et al. (2007), theoretically, two of the oxygens in  $\text{NO}_3^-$  derive from  $\text{H}_2\text{O}$  and one derives from air during microbial nitrification ( $\delta^{18}\text{O}-\text{NO}_3^- = 1/3 \delta^{18}\text{O}-\text{O}_2 + 2/3 \delta^{18}\text{O}-\text{H}_2\text{O}$ ). Our measurements of  $\delta^{18}\text{O}-\text{NO}_3^-$  in the Xin'an River and Lake Qiandao waters (approximately + 2.9 ‰ and + 4.9 ‰, respectively) align closely with a theoretically calculated nitrification range of 1.3 ‰ to 4.3 ‰ (Fig. 5a), indicating that nitrification dominated the  $\text{NO}_3^-$  oxygen isotopic composition during the sampling period. Especially during the high-flow summer season with high temperature, decreased  $\delta^{18}\text{O}-\text{NO}_3^-$  in the Xin'an River might in part attribute to the enhanced mobilization of isotopically lighter nitrate formed by bacterial nitrification processes converting reduced or organic soil nitrogen (Yi et al., 2017). Simultaneously, inputs of organic-rich soil and the oxygen-rich environment in Lake Qiandao supported microbial nitrification. A robust correlation between  $\delta^{18}\text{O}-\text{NO}_3^-$  and  $\delta^{18}\text{O}-\text{H}_2\text{O}$  during the high-flow period (Fig. 5b) also suggested that nitrate isotopic compositions were predominantly shaped by nitrification associated with ambient water rather than soil (Yue et al., 2020). Notably, lake water exhibited higher  $\delta^{18}\text{O}-\text{NO}_3^-$  values compared to river water, which could be attributed to significant lake water evaporation, and the incorporation and exchange of evaporated  $\text{O}-\text{H}_2\text{O}$  into  $\text{NO}_3^-$  during the nitrification process (Hu et al., 2019b).

Additional biological processes within aquatic systems create natural variations in  $\text{NO}_3^-$  isotopic composition. Mechanistic studies have demonstrated that denitrification/assimilation yield a slope ratio of 1:2-1:1 on a plot of the  $\delta^{18}\text{O}$  vs.  $\delta^{15}\text{N}$  of  $\text{NO}_3^-$  (Kendall et al., 2007). Compared with the Xin'an River, Lake Qiandao's extended water residence times facilitated biological transformations of nitrogen to occur (Jiang et al., 2021). Indeed, during the flood season, co-enrichment of  $\delta^{15}\text{N}$  and  $\delta^{18}\text{O}-\text{NO}_3^-$  were evident in Lake Qiandao ( $R^2 = 0.71$ ,  $p < 0.01$ , slope = 1.1) (Fig. 5c). The  $\delta^{15}\text{N}-\text{NO}_3^-$  and  $\delta^{18}\text{O}-\text{NO}_3^-$  versus the logarithm of  $\text{NO}_3^-$ -N ( $\ln(\text{NO}_3^-)$ ) plots also revealed significant negative correlations in Lake Qiandao water (Fig. 5d), indicating the presence of  $\text{NO}_3^-$  removal processes such as dissimilatory nitrate reduction to ammonium (DNRA), assimilation, and denitrification (Kendall et al., 2007; Soto et al., 2019). However, substantial DNRA and denitrification in Lake Qiandao were excluded due to DO concentrations exceeding 6 mg/L (Table S2), a level unresponsive of these anaerobic ( $\text{DO} < 2$  mg/L) processes (Guo et al., 2020; Rivett et al., 2008; Wang, 2020). Moreover, the isotope enrichment factors were approximately 3.0 ‰ for  $\delta^{15}\text{N}-\text{NO}_3^-$  and 5.0 ‰ for  $\delta^{18}\text{O}-\text{NO}_3^-$  (Fig. 5d), falling outside the denitrification range (10 ‰-30 ‰) (Dähnke et al., 2008). Instead, these values aligned with the assimilation range (0.7 ‰-23 ‰) (Granger et al., 2008). Hence, apart from inputs from sources rich in  $\delta^{15}\text{N}-\text{NO}_3^-$  and  $\delta^{18}\text{O}-\text{NO}_3^-$ , such as domestic and animal wastes, as well as leachate from septic tanks,  $\text{NO}_3^-$  assimilation by lake phytoplankton was also the dominant mechanism behind the simultaneous increase of  $\delta^{15}\text{N}-\text{NO}_3^-$  and  $\delta^{18}\text{O}-\text{NO}_3^-$  during the rainy season in lake water (Fig. 5c). In freshwater ecosystems, where dissolved forms of inorganic nitrogen ( $\text{NO}_3^-$ -N and  $\text{NH}_4^+$ -N) are typically assimilated and transformed into organic nitrogen by plants, phytoplankton, and microbes (Yang et al., 2021). The elevated  $\text{NO}_3^-$  concentration from the upstream Xin'an River in July 2020, coupled with longer hydraulic residence time in Lake Qiandao, facilitates the assimilation of nutrients by phytoplankton. Our observations consequently revealed elevated levels of Chla, phytoplankton density, and biomass (Fig. S4b-d). Additionally, we noted the highest suspended particulate matter (SPM) content, with SPOM constituting up to 75 % in July (Figure. S3a). The organic components (SPOM) within SPM represent the organic fractions of phytoplankton, detritus, and bacteria, etc. (Liu et al., 2019). Meanwhile, the lower  $\text{NO}_3^-$ -N concentration (0.34 mg/L) in Lake Qiandao could be in part ascribed to algal uptake, alongside the

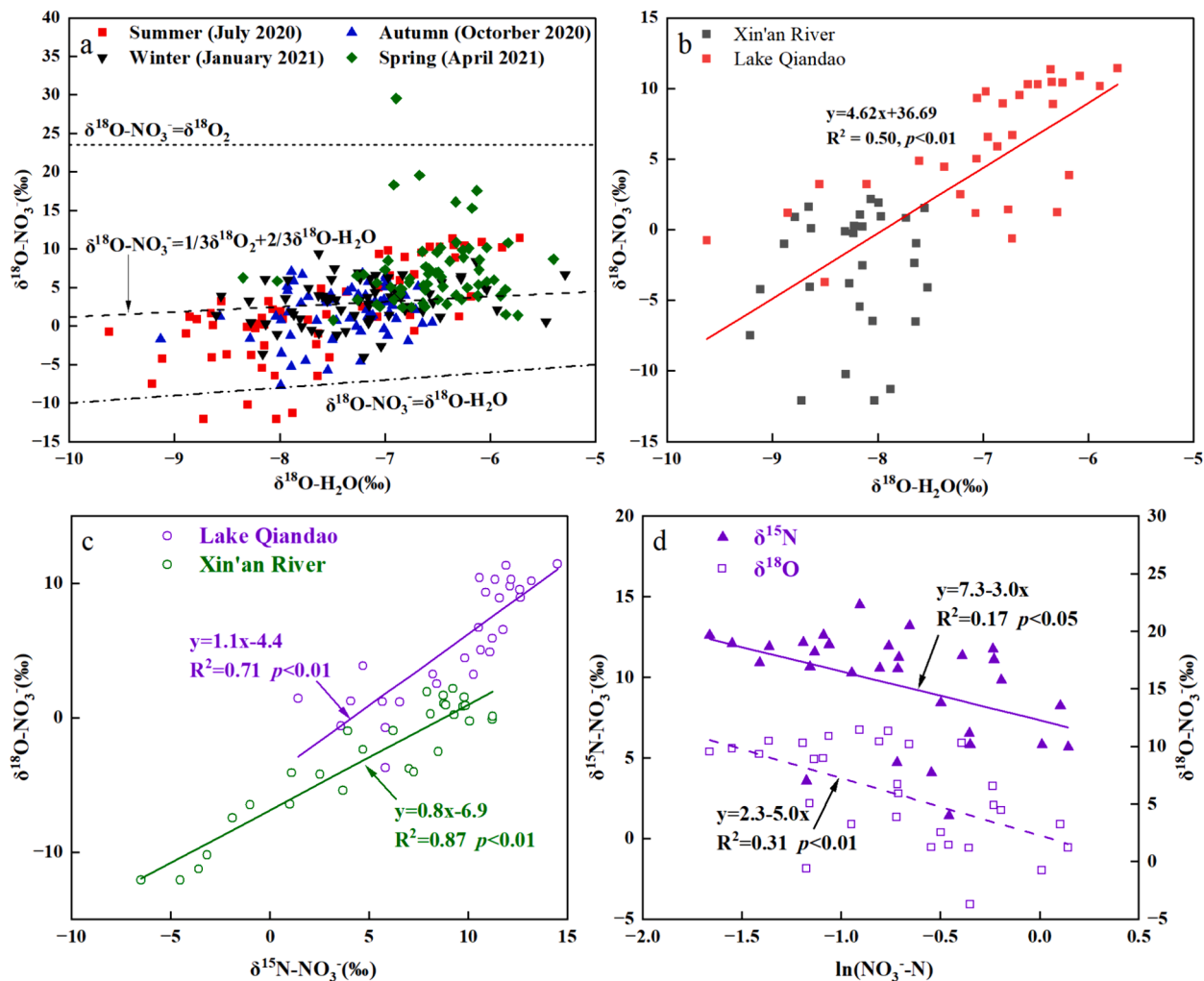


Fig. 5.  $\delta^{18}\text{O}\text{-H}_2\text{O}$  vs.  $\delta^{18}\text{O}\text{-NO}_3^-$  correlation across all seasons (a) and summer specifically (b). Three lines in (a) represent theoretical curves under different conditions. During June 2020 flood period,  $\delta^{15}\text{N}\text{-NO}_3^-$  vs.  $\delta^{18}\text{O}\text{-NO}_3^-$  in the Xin'an River and Lake Qiandao (c); and isotopic compositions vs. logarithmic  $\text{NO}_3^-$ -N concentration in Lake Qiandao (d).

dilution effect from increased water volume. During low flow periods, no significant negative linear correlations were found between  $\delta^{15}\text{N}\text{-NO}_3^-$ ,  $\delta^{18}\text{O}\text{-NO}_3^-$  and  $\ln(\text{NO}_3^-)$  ( $p > 0.05$ ), suggesting limited influence of  $\text{NO}_3^-$  assimilation or denitrification. Instead, the observed dual isotopic behavior was likely driven by conservative mixing of multiple sources.

#### 4.3. Effects of the extreme flooding on nitrate source contributions and isotopic fractionations

Nitrogen cycling, involving nitrification, assimilation, and denitrification, leads to isotopic fractionations that can obscure the original source signal and introduce considerable uncertainty when apportioning nitrate to various sources (e.g., atmospheric deposition, chemical fertilizer, soil N, manure/sewage). Utilizing a robust Bayesian mixing model enables the analysis of mixing fractions and source identification (Zhang et al., 2018). To minimize uncertainty, we systematically evaluated various combinations of sources and fractionation factors to determine the contribution of nitrate sources in both the Xin'an River and Lake Qiandao waters.

During the flood period,  $\text{NO}_3^-$  assimilation processes and isotope fractionation were obviously observed, particularly in Lake Qiandao (Fig. 5). Isotopic fractionation of assimilation was determined from the slope of the relationship between dual nitrate isotopes and  $\ln(\text{NO}_3^-)$  (Eq.

(2)). As shown in Fig. 5d, isotopic enrichment factor ( $\epsilon$ ) values for  $\delta^{15}\text{N}$  and  $\delta^{18}\text{O}$  were 3‰ and 5‰, respectively. We compared the posterior distributions of contributions from the four  $\text{NO}_3^-$  sources in Lake Qiandao for July 2020 in two cases (C1 and C2): one considering the isotopic enrichment factor due to assimilation and the other ignoring it. The results in Fig. S5a-b showed that incorporating the isotopic enrichment factor made the posterior probability distributions of CF and M&S contributions more symmetric and closer to a normal distribution in C2. The mean values of posterior contributions revealed an increase in contributions from SN and CF, while AD and M&S contributions decreased with the incorporation of  $\epsilon$  values (Fig. S5c-d). Notably, apart from the northwestern lake region where soil nitrogen dominated, mirroring results observed in the upstream Xin'an River, all other Lake Qiandao regions consistently featured M&S as the primary contributor, exceeding 40% in each case. In the densely populated southwestern lake region, with a high population density of 233 capita/ $\text{km}^2$ , this proportion increased to 53%.  $\text{NO}_3^-$  pollution primarily originated from point sources of overflow sewage discharged in a diffuse manner, due to incomplete domestic sewage networks and limited treatment capacity. Even during periods of low discharge, M&S retained a significant role ( $36 \pm 5\%$ ) in Lake Qiandao, nearly equaling SN ( $34 \pm 3\%$ ), followed by CF ( $24 \pm 6\%$ ) and AD ( $6 \pm 2\%$ ) (Fig. 6a), which was related to the decreased non-point source due to reduced biological activities and fertilizer application in dry season (Li et al., 2023). Furthermore, CF

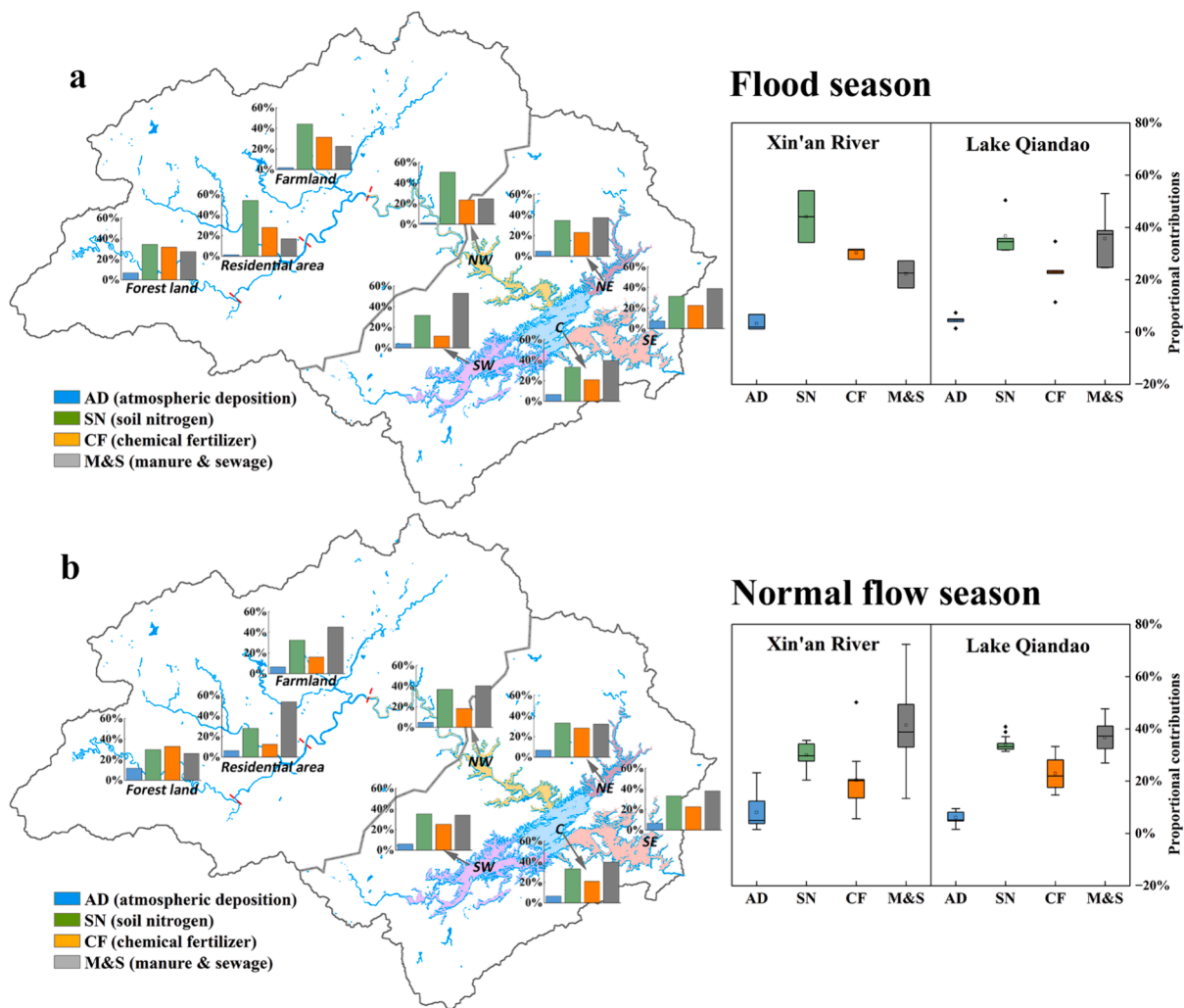


**Fig. 6.** The proportional contributions of different nitrate sources by the SIAR model estimation. NW, NE, SW, SE, and C representing the northwest, northeast, southwest, southeast, and central regions of Lake Qiandao, respectively.

contributed over 25 % of  $\text{NO}_3^-$  in spring, coinciding with intensive nitrification and leaching due to frequent fertilizer application for tea production. This highlighted the need for precise fertilizer management during this period.

During the flood period in Xin'an River, a remarkable feature was the exceptionally high turbidity, with an inorganic suspended particle proportion reaching as high as 85 %, as vividly illustrated in Fig. S6. A significant portion, up to 78 %, of nitrate during this period originated from nonpoint sources (SN, CF, and AD), with SN alone constituting a substantial 44 % to this proportion. Flooding emerged as the primary driving force, leading to an increased inflow of soil particulates and pre-existing  $\text{NO}_3^-$  from the surrounding terrestrial environments flushing into the river. Nitrate derived from microbial uptake, mineralization, and nitrification processes in these submerged soils, serves as a major source to Xin'an River (Kaushal et al., 2011). Furthermore, an elevated M&S contribution occurred during normal flow seasons in upper river (51.9 %) (Fig. 6b), likely attributed to substantial manure application from farmland, a dense population (>161 capita/km<sup>2</sup>), and abundant livestock in residential areas (Zhang et al., 2022).

## 5. Uncertainties and limitations

Our research found that SIAR-derived source contributions align reasonably well with hydrochemical analysis. Nonetheless, several unresolved issues necessitate further investigation and enhancements. In

this study, mean and variance values of two sources (soil nitrogen and chemical fertilizers) were primarily referenced from published literature. Future studies should prioritize acquiring site-specific and more accurate isotope data of N and O isotopes for different sources within the study area. Additionally, considering that SIAR assumes normally distributed sources, the presence of non-normally distributed isotope values may introduce bias. Moreover, as depicted in Fig. S5a-b, posterior distributions of source contributions display wide ranges, suggesting significant uncertainty in the apportionment results. Employing more accurate source information can help mitigate this uncertainty.

## 6. Conclusions

This study investigated the impact of land use changes and a historic summer flooding event on nitrate dynamics and isotopic signatures in the Xin'an River-Lake Qiandao system, a vital water supply for approximately 10 million inhabitants in southeastern China. Human activities and land use significantly influenced nitrate levels and shaped nitrate isotopic patterns. Notably, residential and agricultural areas exhibited the highest nitrate concentrations. Isotopic analysis revealed that flood-induced soil erosion and chemical fertilizers collectively contributed to around 74 % of the nitrate in the Xin'an River, while Lake Qiandao remained impacted by these two non-point sources, contributing 58 % to total nitrogen pollution. However, during flooding, the accumulation of domestic sewage in tributaries, along with overflow

from sewage treatment plants, amplified the contributions of sewage in Lake Qiandao. Furthermore, the relationship between  $\delta^{15}\text{N}\text{-NO}_3^-$  and  $\delta^{18}\text{O}\text{-NO}_3^-$ , alongside elevated levels of Chla and phytoplankton biomass, highlighted the crucial role of nitrification and assimilation in Lake Qiandao, especially during the high-flow summer season. The northwest lake region, acting as a transitional zone with hydraulic connections to upstream rivers, consistently demonstrates isotopic abundance and primary nitrogen sources similar to those found in the upstream Xin'an River basin. This region receives inputs of nutrients and soil particles from upstream, particularly during large and rapid flood events, significantly enhancing nutrient and sediment transport into the reservoir. These findings underscore the importance of water quality management in river-reservoir systems, especially given the increased occurrence of extreme flood events. This encompasses enhanced soil erosion control, precise fertilizer application, and improved wastewater treatment in densely populated regions.

### CRedit authorship contribution statement

**Xingchen Zhao:** Writing – review & editing, Writing – original draft, Visualization, Software, Investigation, Formal analysis. **Hai Xu:** Writing – review & editing, Writing – original draft, Supervision, Resources, Funding acquisition, Conceptualization. **Lijuan Kang:** Investigation, Formal analysis, Data curation. **Guangwei Zhu:** Resources, Investigation, Funding acquisition. **Hans W. Paerl:** Writing – original draft, Resources, Funding acquisition. **Huiyun Li:** Resources, Investigation. **Mingliang Liu:** Resources. **Mengyuan Zhu:** Investigation. **Wei Zou:** Investigation. **Boqiang Qin:** Supervision, Resources. **Yunlin Zhang:** Supervision, Resources.

### Declaration of competing interest

The authors declare that they have no known competing financial interests or personal relationships that could have appeared to influence the work reported in this paper.

### Data availability

Data will be made available on request.

### Acknowledgment

This work was supported by the National Natural Science Foundation of China [42271126]; Nanjing Institute of Geography & Limnology, Chinese Academy of Sciences Foundation [NIGLAS2022GS03]; Natural Science Foundation of Jiangsu [BK20220041]; and US National Science Foundation Projects [1831096, 1803697, 2108917].

### Appendix A. Supplementary data

Supplementary data to this article can be found online at <https://doi.org/10.1016/j.jhydrol.2024.131491>.

### References

Böttcher, J., Strebel, O., Voerkelius, S., Schmidt, H.L., 1990. Using isotope fractionation of nitrate-nitrogen and nitrate-oxygen for evaluation of microbial denitrification in a sandy aquifer. *J. Hydrol.* 114 (3), 413–424.

Chen, F., Lao, Q., Zhang, S., Bian, P., Jin, G., Zhu, Q., Chen, C., 2020b. Nitrate sources and biogeochemical processes identified using nitrogen and oxygen isotopes on the eastern coast of Hainan Island. *Cont. Shelf Res.* 207.

Chen, D., Li, H., Zhang, W., Pueppke, S.G., Pang, J., Diao, Y., 2020a. Spatiotemporal Dynamics of Nitrogen Transport in the Qiandao Lake Basin, a Large Hilly Monsoon Basin of Southeastern China. *Water* 12 (4), 1075.

Chen, N., Wu, J., Hong, H., 2012. Effect of storm events on riverine nitrogen dynamics in a subtropical watershed, southeastern China. *Sci. Total Environ.* 431, 357–365.

Cui, R., Fu, B., Mao, K., Chen, A., Zhang, D., 2020. Identification of the sources and fate of  $\text{NO}_3\text{-N}$  in shallow groundwater around a plateau lake in southwest China using

$\text{NO}_3\text{-isotopes}$  ( $\delta^{15}\text{N}$  and  $\delta^{18}\text{O}$ ) and a Bayesian model. *J. Environ. Manage.* 270, 110897.

Dähnke, K., Bahlmann, E., Emeis, K., 2008. A nitrate sink in estuaries? An assessment by means of stable nitrate isotopes in the Elbe estuary. *Limnol. Oceanogr.* 53 (4), 1504–1511.

Davis, P., Syme, J., Heikoop, J., Fessenden-Rahn, J., Perkins, G., Newman, B., Chrystal, A.E., Hagerty, S.B., 2015. Quantifying uncertainty in stable isotope mixing models. *J. Geophys. Res. Biogeo.* 120 (5), 903–923.

Ding, W., Tsunogai, U., Nakagawa, F., Sambuichi, T., Sase, H., Morohashi, M., Yotsuyanagi, H., 2022. Tracing the source of nitrate in a forested stream showing elevated concentrations during storm events. *Biogeosciences* 19 (13), 3247–3261.

Ding, J., Xi, B., Gao, R., He, L., Liu, H., Dai, X., Yu, Y., 2014. Identifying diffused nitrate sources in a stream in an agricultural field using a dual isotopic approach. *Sci. Total Environ.* 484, 10–18.

Divers, M.T., Elliott, E.M., Bain, D.J., 2014. Quantification of nitrate sources to an urban stream using dual nitrate isotopes. *Environ. Sci. Technol.* 48 (18), 10580–10587.

Galloway, J.N., Dentener, F.J., Capone, D.G., Boyer, E.W., Howarth, R.W., Seitzinger, S. P., Asner, G.P., Cleveland, C.C., Green, P.A., Holland, E.A., Karl, D.M., Michaels, A. F., Porter, J.H., Townsend, A.R., Vöösmary, C.J., 2004. Nitrogen cycles: past, present, and future. *Biogeochemistry* 70 (2), 153–226.

Gonfiantini, R., 1986. Chapter 3 - Environmental Isotopes in Lake Studies. In: Fritz, P., Fontes, J.C. (Eds.), *The Terrestrial Environment*, B. Elsevier, Amsterdam, pp. 113–168.

Graf, W.L., Wohl, E., Sinha, T., Sabo, J.L., 2010. Sedimentation and sustainability of western American reservoirs. *Water Resour. Res.* 46 (12), W12535.

Granger, J., Wankel, S.D., 2016. Isotopic overprinting of nitrification on denitrification as a ubiquitous and unifying feature of environmental nitrogen cycling. *Proc. Natl. Acad. Sci. Unit. States Am* 113 (42), E6391–E6400.

Granger, J., Sigman, D.M., Lehmann, M.F., Tortell, P.D., 2008. Nitrogen and oxygen isotope fractionation during dissimilatory nitrate reduction by denitrifying bacteria. *Limnol. Oceanogr.* 53 (6), 2533–2545.

Grill, G., Lehner, B., Thieme, M., Geenen, B., Tickner, D., Antonelli, F., Babu, S., Borrelli, P., Cheng, L., Crochetiere, H., Ehalt Macedo, H., Filgueiras, R., Goichot, M., Higgins, J., Hogan, Z., Lip, B., McClain, M.E., Meng, J., Mulligan, M., Nilsson, C., Olden, J.D., Opperman, J.J., Petry, P., Reidy Liermann, C., Sáenz, L., Salinas-Rodríguez, S., Schelle, P., Schmitt, R.J.P., Snider, J., Tan, F., Tockner, K., Valdujo, P. H., van Soesbergen, A., Zarfl, C., 2019. Mapping the world's free-flowing rivers. *Nature* 569 (7755), 215–221.

Guo, X., Tang, Y., Xu, Y., Zhang, S., Ma, J., Xiao, S., Ji, D., Yang, Z., Liu, D., 2020. Using stable nitrogen and oxygen isotopes to identify nitrate sources in the Lancang River, upper Mekong. *J. Environ. Manage* 274, 111197.

Guo, C., Zhu, G., Qin, B., Zhang, Y., Zhu, M., Xu, H., Chen, Y., Paerl, H.W., 2019. Climate exerts a greater modulating effect on the phytoplankton community after 2007 in eutrophic Lake Taihu, China: Evidence from 25 years of recordings. *Ecol. Indic.* 105, 82–91.

Ho, J.C., Michalak, A.M., Pahlevan, N., 2019. Widespread global increase in intense lake phytoplankton blooms since the 1980s. *Nature* 574 (7780), 667–670.

Hu, M., Liu, Y., Zhang, Y., Dahlgren, R.A., Chen, D., 2019a. Coupling stable isotopes and water chemistry to assess the role of hydrological and biogeochemical processes on riverine nitrogen sources. *Water Res.* 150, 418–430.

Hu, M., Wang, Y., Du, P., Shui, Y., Cai, A., Lv, C., Bao, Y., Li, Y., Li, S., Zhang, P., 2019b. Tracing the sources of nitrate in the rivers and lakes of the southern areas of the Tibetan Plateau using dual nitrate isotopes. *Sci. Total Environ.* 658, 132–140.

Jiang, H., Ma, J., Xu, H., Xu, Z., Liu, W., Pan, K., 2021. Multiple isotopic compositions reveal complex nitrogen cycling in a subtropical estuary. *Environ. Pollut.* 272, 116410.

Jin, Z., Qin, X., Chen, L., Jin, M., Li, F., 2015. Using dual isotopes to evaluate sources and transformations of nitrate in the West Lake watershed, eastern China. *J. Contam. Hydrol.* 177–178, 64–75.

Jin, Z., Cen, J., Hu, Y., Li, L., Shi, Y., Fu, G., Li, F., 2019. Quantifying nitrate sources in a large reservoir for drinking water by using stable isotopes and a Bayesian isotope mixing model. *Environ. Sci. Pollut. Res. Int.* 26 (20), 20364–20376.

Jin, X., Tu, Q., 1990. *Standard of Lake Eutrophication survey of China*. China Environmental Science Publishing House, Beijing.

Kaushal, S.S., Groffman, P.M., Band, L.E., Elliott, E.M., Shields, C.A., Kendall, C., 2011. Tracking nonpoint source nitrogen pollution in human-impacted watersheds. *Environ. Sci. Technol.* 45 (19), 8225–8232.

Kendall, C., 1998. Chapter 16 - Tracing nitrogen sources and cycling in catchments. In: Kendall, C., McDonnell, J.J. (Eds.), *Isotope Tracers in Catchment Hydrology*. Elsevier, Amsterdam, pp. 519–576.

Kendall, C., Elliott, E.M., Wankel, S.D., 2007. Tracing anthropogenic inputs of nitrogen to ecosystems, in: Michener, R., Lajtha, K. (Eds.), *Stable Isotopes in Ecology and Environmental Science*, pp. 375–449.

Keys, T.A., Caudill, M.F., Scott, D.T., 2019. Storm effects on nitrogen flux and longitudinal variability in a river-reservoir system. *River Res. Appl.* 35, 577–586.

Kondolf, G.M., Gao, Y., Annandale, G.W., Morris, G.L., Jiang, E., Zhang, J., Cao, Y., Carling, P., Fu, K., Guo, Q., Hotchkiss, R., Peteuil, C., Sumi, T., Wang, H.-W., Wang, Z., Wei, Z., Wu, B., Wu, C., Yang, C.T., 2014. Sustainable sediment management in reservoirs and regulated rivers: Experiences from five continents. *Earth's Future* 2 (5), 256–280.

Li, S., Goldberg, M.D., Sjöberg, W., Zhou, L., Nandi, S., Chowdhury, N., Straka, W., Yang, T., Sun, D., 2020a. Assessment of the catastrophic Asia floods and potentially affected population in summer 2020 using VIIRS flood products. *Remote Sens. (Basel)* 12 (19), 3176.

- Li, Y., Shi, K., Zhang, Y., Zhu, G., Zhang, Y., Wu, Z., Liu, M., Guo, Y., Li, N., 2020b. Analysis of water clarity decrease in Xin'anjiang Reservoir, China, from 30-Year Landsat TM, ETM+, and OLI observations. *J. Hydrol.* 590, 125476.
- Li, Y., Li, L., Sun, W., Yin, X., 2021. Nitrate sources and transformations along a mountain-to-plain gradient in the Taizi River basin in Northeast China. *Environ. Sci. Pollut. Res.* 28 (41), 58284–58297.
- Li, H., Yu, C., Qin, B., Li, Y., Jin, J., Luo, L., Wu, Z., Shi, K., Zhu, G., 2022. Modeling the effects of climate change and land use/land cover change on sediment yield in a large reservoir basin in the East Asian monsoonal region. *Water* 14 (15), 2346.
- Li, C., Yue, F.-J., Zhong, J., Xu, S., Li, S.-L., 2023. Hydrological regulation of nitrate sources, transformation and transport pathway in a karstic river. *J. Hydrol.* 617.
- Liu, D., Duan, H., Yu, S., Shen, M., Xue, K., 2019. Human-induced eutrophication dominates the bio-optical compositions of suspended particles in shallow lakes: Implications for remote sensing. *Sci. Total Environ.* 667, 112–123.
- Mariotti, A., Lancelot, C., Billen, G., 1984. Natural isotopic composition of nitrogen as a tracer of origin for suspended organic matter in the Scheldt estuary. *Geochim. Cosmochim. Acta* 48 (3), 549–555.
- McIlvin, M.R., Altabet, M.A., 2005. Chemical conversion of nitrate and nitrite to nitrous oxide for nitrogen and oxygen isotopic analysis in freshwater and seawater. *Anal. Chem.* 77 (17), 5589–5595.
- Mueller, C., Zink, M., Samaniego, L., Krieg, R., Merz, R., Rode, M., Knoller, K., 2016. Discharge driven nitrogen dynamics in a mesoscale river basin as constrained by stable isotope patterns. *Environ. Sci. Technol.* 50 (17), 9187–9196.
- Neville, J.A., Emanuel, R.E., Nichols, E.G., Vose, J., 2021. Extreme flooding and nitrogen dynamics of a blackwater river. *Water Resour. Res.* 57 (12), e2020WR029106.
- Nieder, R., Benbi, D.K., Reichl, F.X., 2018. Reactive water-soluble forms of nitrogen and phosphorus and their impacts on environment and human health. In: Nieder, R., Benbi, D.K., Reichl, F.X. (Eds.), *Soil Components and Human Health*. Springer, Netherlands, Dordrecht, pp. 223–255.
- Parnell, A.C., Inger, R., Bearhop, S., Jackson, A.L., 2010. Source partitioning using stable isotopes: coping with too much variation. *PLoS One* 5 (3), e9672.
- Pueppke, S.G., Zhang, W., Li, H., Chen, D., Ou, W., 2019. An integrative framework to control nutrient loss: insights from Two Hilly Basins in China's Yangtze River Delta. *Water* 11 (10), w11102036.
- Qin, B., Deng, J., Shi, K., Wang, J., Brookes, J., Zhou, J., Zhang, Y., Zhu, G., Paerl, H.W., Wu, L., 2021. Extreme climate anomalies enhancing cyanobacterial blooms in eutrophic Lake Taihu, China. *Water Resour. Res.* 57 (7), e2020WR029371.
- Rivett, M.O., Buss, S.R., Morgan, P., Smith, J.W.N., Bement, C.D., 2008. Nitrate attenuation in groundwater: A review of biogeochemical controlling processes. *Water Res.* 42 (16), 4215–4232.
- Seneviratne, S.I., X. Zhang, M. Adnan, W. Badi, C. Dereczynski, A. Di Luca, S. Ghosh, I. Iskandar, J. Kossin, S. Lewis, F. Otto, I. Pinto, M. Satoh, S.M. Vicente-Serrano, M. Wehner, and B. Zhou, 2021. Weather and Climate Extreme Events in a Changing Climate, in: Masson-Delmotte, Zhai, V.P., Pirani, A., Connors, S.L., Péan, C., Berger, S., Caud, N., Chen, Y., Goldfarb, L., Gomis, M.I., Huang, M., Leitzell, K., Lonnoy, E., Matthews, J.B.R., Maycock, T.K., Waterfield, T., O. Yelekçi, Yu, R., Zhou, B. (Eds.), *Climate Change 2021: The Physical Science Basis. Contribution of Working Group I to the Sixth Assessment Report of the Intergovernmental Panel on Climate Change*, Cambridge University Press, pp. 1513–1766.
- Soto, D.X., Koehler, G., Wassenaar, L.I., Hobson, K.A., 2019. Spatio-temporal variation of nitrate sources to Lake Winnipeg using N and O isotope ( $\delta^{15}\text{N}$ ,  $\delta^{18}\text{O}$ ) analyses. *Sci. Total Environ.* 647, 486–493.
- Voss, M., Deutsch, B., Elmgren, R., Humborg, C., Kuoppo, P., Pastuszak, M., Rolff, C., Schulte, U., 2006. Source identification of nitrate by means of isotopic tracers in the Baltic Sea catchments. *Biogeosciences* 3 (4), 663–676.
- Wang, F., 2020. Impact of a large sub-tropical reservoir on the cycling of nutrients in a river. *Water Res.* 186, 116363.
- Wang, Y., Peng, J., Cao, X., Xu, Y., Yu, H., Duan, G., Qu, J., 2020. Isotopic and chemical evidence for nitrate sources and transformation processes in a plateau lake basin in Southwest China. *Sci. Total Environ.* 711, 134856.
- Wang, S., Wang, A., Yang, D., Gu, Y., Tang, L., Sun, X., 2023. Understanding the spatiotemporal variability in nonpoint source nutrient loads and its effect on water quality in the upper Xin'an river basin, Eastern China. *J. Hydrol.* 621, 129582.
- Xia, Y., Li, Y., Zhang, X., Yan, X., 2017. Nitrate source apportionment using a combined dual isotope, chemical and bacterial property, and Bayesian model approach in river systems. *J. Geophys. Res. Biogeo.* 122 (1), 2–14.
- Xia, X., Li, S., Wang, F., Zhang, S., Fang, Y., Li, J., Michalski, G., Zhang, L., 2019. Triple oxygen isotopic evidence for atmospheric nitrate and its application in source identification for river systems in the Qinghai-Tibetan Plateau. *Sci. Total Environ.* 688, 270–280.
- Xue, D., Botte, J., De Baets, B., Accoe, F., Nestler, A., Taylor, P., Van Cleemput, O., Berglund, M., Boeckx, P., 2009. Present limitations and future prospects of stable isotope methods for nitrate source identification in surface- and groundwater. *Water Res.* 43 (5), 1159–1170.
- Xue, D., De Baets, B., Van Cleemput, O., Hennessy, C., Berglund, M., Boeckx, P., 2012. Use of a Bayesian isotope mixing model to estimate proportional contributions of multiple nitrate sources in surface water. *Environ. Pollut.* 161, 43–49.
- Yang, L., Han, J., Xue, J., Zeng, L., Shi, J., Wu, L., Jiang, Y., 2013. Nitrate source apportionment in a subtropical watershed using Bayesian model. *Sci. Total Environ.* 463–464, 340–347.
- Yang, Y.Y., Toor, G.S., 2016.  $\delta^{15}\text{N}$  and  $\delta^{18}\text{O}$  reveal the sources of nitrate-nitrogen in urban residential stormwater runoff. *Environ. Sci. Technol.* 50 (6), 2881–2889.
- Yang, N., Zhang, C., Wang, L., Li, Y., Zhang, W., Niu, L., Zhang, H., Wang, L., 2021. Nitrogen cycling processes and the role of multi-trophic microbiota in dam-induced river-reservoir systems. *Water Res.* 206, 117730.
- Yi, Q., Chen, Q., Hu, L., Shi, W., 2017. Tracking nitrogen sources, transformation, and transport at a basin scale with complex plain river networks. *Environ. Sci. Technol.* 51 (10), 5396–5403.
- Yin, C., Yang, H., Wang, J., Guo, J., Tang, X., Chen, J., 2020. Combined use of stable nitrogen and oxygen isotopes to constrain the nitrate sources in a karst lake. *Agr. Ecosyst. Environ.* 303, 107089.
- Yue, F.J., Li, S.L., Waldron, S., Wang, Z.J., Oliver, D.M., Chen, X., Liu, C.Q., 2020. Rainfall and conduit drainage combine to accelerate nitrate loss from a karst agroecosystem: Insights from stable isotope tracing and high-frequency nitrate sensing. *Water Res.* 186, 116388.
- Zhang, P., Chen, L., Yan, T., Liu, J., Shen, Z., 2022. Sources of nitrate-nitrogen in urban runoff over and during rainfall events with different grades. *Sci. Total Environ.* 808, 152069.
- Zhang, Y., Li, F., Zhang, Q., Li, J., Liu, Q., 2014. Tracing nitrate pollution sources and transformation in surface- and ground-waters using environmental isotopes. *Sci. Total Environ.* 490, 213–222.
- Zhang, M., Zhi, Y., Shi, J., Wu, L., 2018. Apportionment and uncertainty analysis of nitrate sources based on the dual isotope approach and a Bayesian isotope mixing model at the watershed scale. *Sci. Total Environ.* 639, 1175–1187.
- Zhou, Y., Liu, M., Zhou, L., Jang, K.S., Xu, H., Shi, K., Zhu, G., Liu, M., Deng, J., Zhang, Y., Spencer, R.G.M., Kothawala, D.N., Jeppesen, E., Wu, F., 2020. Rainstorm events shift the molecular composition and export of dissolved organic matter in a large drinking water reservoir in China: High frequency buoys and field observations. *Water Res.* 187, 116471.
- Zhu, G., Cheng, X., Wu, Z., Shi, P., Zhu, M., Xu, H., Guo, C., Zhao, X., 2022. Spatio-temporal variation of nutrient concentrations and environmental challenges of Qiandaohu Reservoir, China. *Res. Environ. Sci.* 35 (4), 852–863.